Control and Cybernetics

vol. **47** (2018) No. 1

On representative functions method for clustering of 2D contours with application to pottery fragments typology*

by

Agnieszka Kaliszewska[1] **and Monika Syga**[2]

[1]Systems Research Institute, Polish Academy of Sciences,
Newelska 6, 01-447 Warszawa, Poland,
Agnieszka.Kaliszewska@ibspan.waw.pl
[2] Warsaw University of Technology, Faculty of Mathematics and Information Science, Koszykowa 75, 00-662 Warsaw, Poland,
M.Syga@mini.pw.edu.pl

Abstract: We investigate clustering of 2D contours which represent cross-sections of rotationally symmetric objects. We propose modifications of the existing representations of digitized 2D contours and similarity measures. In particular, we represent each of the investigated objects as a single number and two functions and we use the DTW distance to measure their similarity. We apply our method to clustering of pottery fragments.

Keywords: shape representation, 2D contours, cross-sections, rotationally symmetric objects, representative functions, clustering, dynamic time warping (DTW) distance

1. Introduction

The paper concerns clustering analysis of 2D contours. This topic has been investigated in, e.g., Cao (2003); Forsyth, Mundy, di Gesu and Cipolla (1999); Bandyopadhyay, Saha (2013) and Kłopotek and Wierzchoń (2015). To perform a complete cluster analysis of a given set of shapes (2D contours) one should choose appropriate tools and methods for each of the three main steps: (*i*) shape representation, (*ii*) similarity (dissimilarity) measure, (*iii*) clustering algorithm, see, e.g., Kłopotek and Wierzchoń (2015). The choice made at each of these steps influences in an essential manner the results of the clustering.

In this paper we concentrate mainly on the first two steps, i.e. on shape representation and on similarity measures, related to 2D contours. There exist a lot of methods of representing 2D contours and defining their similarity (dissimilarity).

The choice of the appropriate methods for (*i*) and (*ii*) depends heavily on the application to which they refer e.g. script recognition, see Ghosh, Dube

*Submitted: June 2018; Accepted: August 2018.

and Shivaprasad (2010); Masood and Safraz (2009); Yadav and Yadav (2015), analysis of stock market trends, see Parracho, NEVES and Horta (2010), protein shape matching, see Binkowski and Joachimiak (2008), or speech recognition, see Bridle (1980).

In the investigated application, the 2D contours are boundaries of cross-sections of rotationally symmetric objects, i.e. a special class of 2D curves. A particular feature of the considered sets of the curves is that they are to be grouped with respect to subtle differences between them. Hence, both the shape representation and the similarity measure should recognize such differences between the curves.

1.1. The aim

The aim of this paper is to investigate the representations and similarity measures for 2D curves, which are the boundaries of cross-sections of rotationally symmetric objects (objects of revolution). Our approach is based on the analysis and the modification of the existing schemes, given in Gilboa, Karasik, Sharon and Smilansky (2004) and Karasik and Smilansky (2001, 2008).

The proposed modifications focus on efficient representations of the curves, and on similarity measures, which improve the clustering results. In the present work we do not focus on clustering method, we merely apply hierarchical clustering method as available in standard packages.

Since for such curves there are no benchmark data, in order to provide trustworthy comparisons we apply the proposed methodological modifications to data coming from the same domain as in Gilboa, Karasik, Sharon and Smilansky (2004), Karasik and Smilansky (2001, 2008), that is - archaeological pottery.

1.2. Shape representations and similarity measures

Shape representation (shape description) methods can be divided into three main categories: contour based, silhouette based and skeleton based, see Arica and Yarman-Vural (2003). Among the most frequently used shape representation methods let us mention the following:

1. Aligning curve (Sebastian, Klein and Kimia, 2003),
2. K-curvature (Arica and Yarman-Vural, 2003),
3. Shape context (Belongie and Malik, 2002, 2000),
4. Bézier curves (Masood and Safraz, 2009; Sarfaz, Masood and Asim, 2004; Pal, Ganguly and Biswas, 2007; Masood and Sarfraz, 2008; Sarfaz and Masood, 2007),
5. Skeletal representation (Kimmel, Shaked, Kiryati and Bruckstein, 1995),
6. Fourier descriptors (Rui, She and Huang, 1996; Zhang and Lu, 2002),
7. Representative functions (Karasik and Smilansky, 2001; Sragusti, Karasik, Sharon and Smilansky, 2005; Karasik and Smilansky, 2008).

Evaluations and comparisons of different shape descriptors are given in, e.g., Amanatiadis, Kaburlasos, Gasteratos and Papadatis (2011), García-Ordás, Ale-

gre, García-Olalla and García-Ordás (2013). In the present paper, the shapes are represented with the use of representative functions.

In the literature, a number of similarity measures for curves are used. Usually, the following measures are used as distances between curves:

1. Hausdorff distance (Aronov, Har-Peled, Knauer, Wang and Wenk, 2006),
2. Fréchet distance (Aronov, Har-Peled, Knauer, Wang and Wenk, 2006; Wylie, 2013; Wylie and Zhu, 2016),
3. Euclidean distance (Kłopotek and Wierzchoń, 2015).

Other classical similarity measures are discussed in Kłopotek and Wierzchoń (2015). We are using a similarity measure based on the Euclidean distance.

1.3. The organization of the paper

The organization of the paper is as follows. In Section 2 we describe the class of investigated 2D curves.

In Section 3 we discuss the analytical and discrete representations of 2D curves. Then, in Section 4 we describe the adopted similarity measures. In Section 5 we present the representative functions method. In Section 6 we describe the archaeological objects, on which we test our method. In Section 7 we present the results of the numerical experiments and the discussion. Section 8 concludes the paper.

2. The class of investigated objects

Formally, our aim is to classify 2D regular open curves $\alpha \subset \mathbb{R}^2$.

Each curve is a function $\alpha : [t_0, t_1] \to \mathbb{R}^2$ represented as

$$\alpha(t) := (x(t), y(t)) \quad t \in [t_0, t_1],$$

where $x : [t_0, t_1] \to \mathbb{R}$, and $y : [t_0, t_1] \to \mathbb{R}$ are twice differentiable real-valued functions. The curve is called *regular* when its derivative is nonzero at each point, i.e. $\alpha'(t) := (x'(t), y'(t)) \neq (0, 0)$ for each $t \in [t_0, t_1]$.

In the present paper we take advantage of the fact that our curves come from technical drawings, that is, the drawings, which are all made according to a fixed set of strict rules and are drawn so as to visually communicate how the objects are constructed.

In consequence, the curves (data) are given in a standardized form, i.e. they are not prone to randomness as to their location within the coordinate system OXY.

First of all, these curves are outlines of cross-sections of objects of revolution, with the axis OY fixed as the rotation axis. Each curve is located in the first quadrant of the plane in the way visualized in Fig. 4. For technical reasons each cross-section is put in the first quadrant upside down. In consequence, its uppermost points become the lowermost, and are forced to lay on the axis

OX. The point $(x_r, 0)$ with the smallest value of x-coordinate corresponding to y-coordinate $y = 0$ defines the *the radius r of the rotating object of revolution*,

$$r := x_r \tag{1}$$

the object being the result of the rotation of the curve around the axis OY.

The technical drawings, from which the curves are generated, represent the objects in the same scale. This ensures that the information about the proportions between the objects (and consequently, the curves) is maintained. Moreover, we assume that a large number of investigated objects are represented only partially, i.e. a given curve may not represent the entire object, but only a part of it. However, we assume that the uppermost part of the contour is known, i.e. we are able to find the radius x_r.

We want to perform a clustering, i.e. an unsupervised classification of sets of curves described above, with respect to their size, global shape and local shape. Since, as mentioned before, the curves represent the same class of objects (cross-sections of rotational 3D objects), we are looking for subtle differences within the investigated set. This is in contrast to many other problems, considered in literature, where the objects differ significantly, e.g. represent animals and/or geometric figures. The subtle differences are of great importance to us, as a relatively small change in the curve might have important implications for the shape of the object of revolution represented by it. A similar problem has been considered in Chapter 4 of Ramsay and Silverman (2002).

It is worth mentioning that papers concerning a complete process of clustering analysis of this kind of objects are rather seldom, see, e.g., Cao and Mumford (2002); Mumford (1991); Sharon and Mumford (2006), and the references therein.

3. Representations of 2D curves

There exist numerous ways of analysing 2D shapes and curves, see, e.g., Sharon and Mumford (2006); Zhang and Lu (2003, 2004), and the references therein.

The boundary of each silhouette, i.e. a 2D object, is represented as a curve $\alpha(t) = (x(t), y(t))$, $t \in [t_1, t_2]$. For the derivative vector α' we have $\alpha'(t) = (x'(t), y'(t))$.

3.1. Analytical representation of 2D curves

Each curve can be parameterized by the arc length s, defined as

$$s(t) = \int_{t_0}^{t} |\alpha'(u)| \mathrm{d}u. \tag{2}$$

With this parameterization, the curve can be written down as

$$\alpha(s) = (x(s), y(s)) \quad s \in [s_0, s_1]. \tag{3}$$

Let us note that the value $|x(s)|$ equals the Euclidean distance of $(x(s), y(s))$ to the rotation axis $0Y$. Since the curves we are investigating are located in the first quadrant, we have

$$|x(s)| = x(s). \tag{4}$$

Let $\theta(s)$ be the angle, which $\alpha'(s)$ forms with the positive x-axis, measured anti-clockwise from the positive x-axis to $\alpha'(s)$. The function tangent $\theta(s)$ is then defined in the following way

$$\theta(s) := \arctan\left(\frac{y'(s)}{x'(s)}\right). \tag{5}$$

Now, note that the matrix $J = \begin{bmatrix} 0 & -1 \\ 1 & 0 \end{bmatrix}$ acts on $\mathbb{R}^2$ by rotating vectors anti-clockwise by the angle of $\pi/2$.

The curvature function κ is defined as follows

$$\kappa(s) := \alpha''(s)J(\alpha'(s)). \tag{6}$$

We have the following relationship between the tangent and curvature functions

$$\kappa(s) = \theta'(s). \tag{7}$$

The following fundamental theorem holds.

THEOREM 1 (DO CARMO, 1976) *Suppose we are given two vectors $a, b \in \mathbb{R}^2$, $b \neq 0$ and a continuous function $\kappa : [t_0, t_1] \to \mathbb{R}$. Then there exists a unique curve $\alpha : [t_0, t_1] \to \mathbb{R}^2$ parameterized by arc length with curvature function κ, initial position $\alpha(t_0) = a$ and initial direction $\alpha'(t_0) = b$.*

Theorem 1 shows the importance of the curvature function in identifying the curve. By Theorem 1, two vectors a, and b, and the curvature function κ suffice to describe uniquely a given curve α. The role of the first and the second derivatives $\theta(s)$ and $\kappa(s)$, respectively, in functional data analysis has been extensively discussed in Chapters 18 and 19 of Ramsay and Silverman (2002).

On the other hand, from the computational point of view, the formulas (5) and (7) may not perform well and may be sensitive to perturbations due to numerical differentiation errors and noise, see Kovalevsky (2001); Liu, Latecki, and Liu (2008).

Taking into account these observations, in order to minimize the impact of the imprecisions mentioned, when considering the problem of clustering of our class of 2D curves (Section 2), we use the following two representations of investigated curves:

R1: arc-length $x(s)$ given by (4), the tangent $\theta(s)$ from (5), and the curvature $\kappa(s)$ from (7);

R2: the radius r given by (1), the tangent $\theta(s)$ from (5), and the curvature $\kappa(s)$ from (7).

Some illustrations for the representation of curves using $\theta(s)$ and $\kappa(s)$ are provided in Figs 1 through 3.

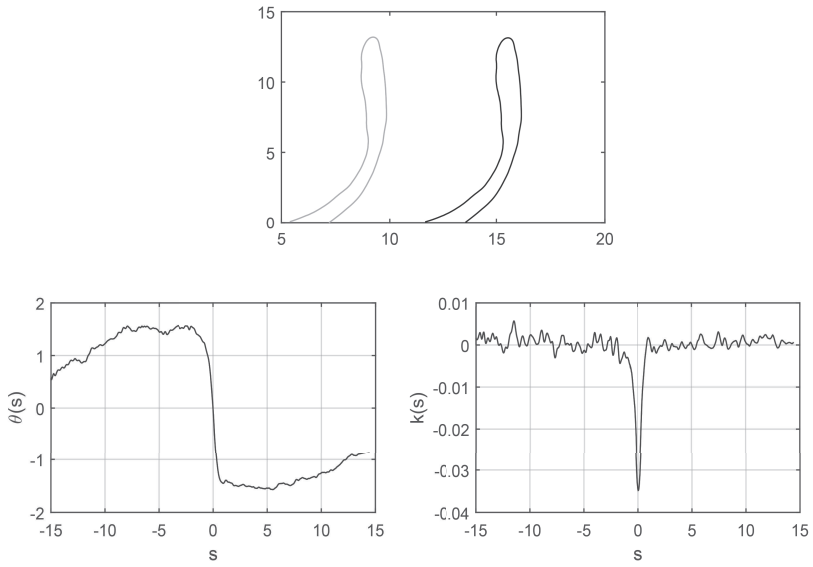

Figure 1: Profiles featuring the same shape but different radius

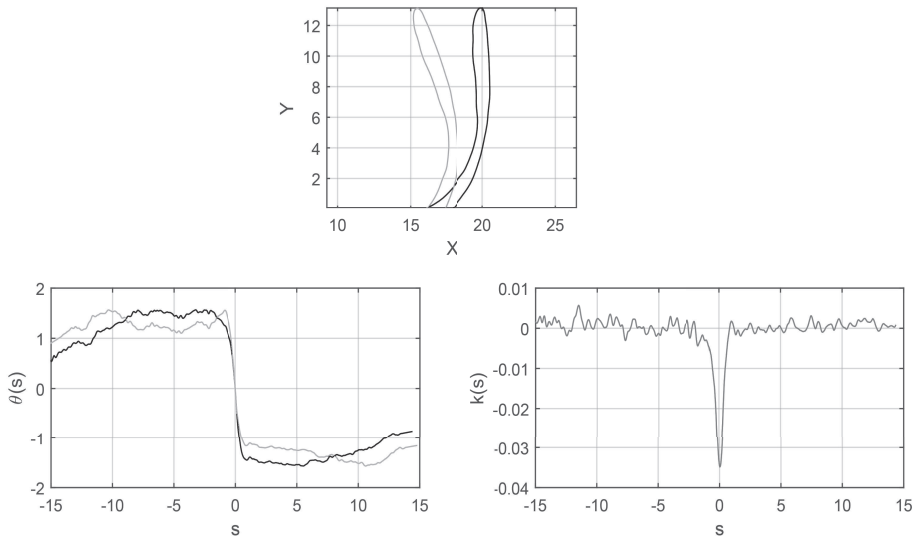

Figure 2: Profiles featuring the same local shape but their global shapes are different

3.2. Discrete representation of the 2D curves

In practice, the hand-made technical drawings are digitized, the contours (boundaries) are extracted and smoothed with the help of standard MatLab boundary

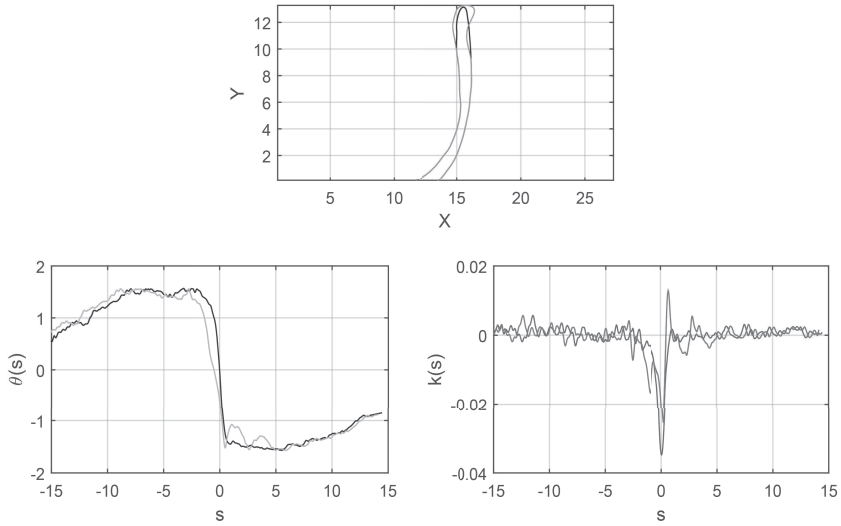

Figure 3: Profiles featuring different global shapes

extraction techniques. In further analysis, we consider discrete curves, i.e. a given curve α is a pair of vectors,

$$\alpha := (\bar{x}, \bar{y}) = (x(i), y(i)),\ i = 1, ..., k_\alpha.$$

These discrete curves are parameterized by the arc length function s, where $s = 0$ is the starting point, which is chosen so as to correspond to the lowermost point of the curve with the smallest value of x-coordinate, i.e. $x(0) = x_r = r$ is the radius of the object (see Fig. 4).

The arc length function s, defined in (2), is calculated with the help of numerical differentiation and numerical integration procedures.

We consider three functions, which represent the shapes of the discrete curves in $\mathbb{R}^2$. The tangent $\theta(s)$ and the curvature $\kappa(s)$ functions are defined in Subsection 3.1, and are calculated numerically for discrete curves. Apart from these two functions, we also use the $x(s)$ function, which is the distance of the point s from the Y axis. This function is used in order to preserve the information about the radius of the object.

According to Theorem 1, in order to describe uniquely a curve we need only the curvature function, but the numerical calculation of the curvature function of discrete curves may not be precise (Kovalevsky, 2001), due to the loss of information during the digitization of the image and involvement of the second derivative. In order to minimize the impact of these imprecisions in the description of the shape we also use the tangent function.

From the formal point of view, the following representations of our curves

can be taken into account in the clustering analysis:

1. R1d - full description of the curve consisting of three vectors: $x(s)$, $\theta(s)$, $\kappa(s)$
2. R2d - description of the curve consisting of two vectors: $\theta(s)$, $\kappa(s)$ and a single number x_r, representing the radius of rotation (see Fig. 1)

The discrete representation R1d has been already considered in Gilboa, Karasik, Sharon and Smilansky (2004), Karasik and Smilansky (2001, 2008). Representation R2d is new and will be analysed in Section 7. According to Theorem 1 the following representation R3d is also conceivable:

3. R3d - description of the curve consisting of a single vector $\kappa(s)$ and: x_r, representing the radius, and $\theta(r)$, representing the initial tangent vector.

Preliminary tests on exploiting R3 are discouraging. The reason is that $\theta(r)$, together with x_r and the curvature function $\kappa(s)$ suffice to uniquely describe a curve, but they do not suffice to properly compare two curves to each other.

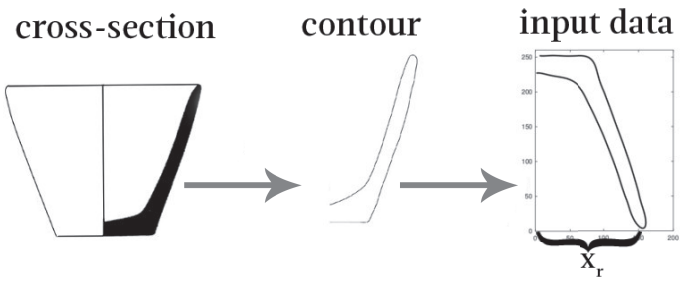

Figure 4: The transformation of a section of a rotationally symetric object into a 2D input data curve

4. Similarity measures

Now we discuss some measures of similarities and dissimilarities between curves. To achieve this, we define the "distance" between curves using the functions $\theta(s)$, $\kappa(s)$, and the function $x(s)$ or radius x_r. We calculate this distance in two different ways.

4.1. Euclidean similarity

In this section, in order to establish the distance between curves we use a standard definition of distance between the functions. Let f, g be two arbitrary functions, then

$$d(f,g) = \sqrt{\frac{1}{L}\int_{S_{\min}}^{S_{\max}} (f(s)-g(s))^2 \mathrm{d}s}. \tag{8}$$

The functions, which will be compared using the formula (8), are usually defined on different intervals on the s axis, so the interval $[S_{min}, S_{max}]$ is taken as the shorter of the domains of functions f, g, and L is the length of the interval $[S_{min}, S_{max}]$.

It is clear that since we work with discrete curves, the numbers $d(\cdot,\cdot)$ are calculated in the discrete way, i.e. by using the finite sum. The distance between functions vanishes if and only if they are identical.

In order to establish the comparison between curves i and j without bias, we introduce a normalization factor: the averages of respective functions over the set of curves considered, with the set comprising M curves:

$$\langle x\rangle = \frac{1}{M}\sum_{i=1}^{M}\sqrt{\frac{1}{L_i}\int_{S^i_{\min}}^{S^i_{\max}}(x_i(s))^2\mathrm{d}s}$$

$$\langle \theta\rangle = \frac{1}{M}\sum_{i=1}^{M}\sqrt{\frac{1}{L_i}\int_{S^i_{\min}}^{S^i_{\max}}(\theta_i(s))^2\mathrm{d}s}$$

$$\langle \kappa\rangle = \frac{1}{M}\sum_{i=1}^{M}\sqrt{\frac{1}{L_i}\int_{S^i_{\min}}^{S^i_{\max}}(\kappa_i(s))^2\mathrm{d}s},$$

where L_i is the length of the interval $[S^i_{min}, S^i_{max}]$, for $i = 1, ..., M$.

Now we define the distance between the curves i and j as the sum weighted of normalized distances of the three functions:

$$d(i,j) = \frac{\omega_x}{\langle x\rangle}d(x_i,x_j) + \frac{\omega_\theta}{\langle\theta\rangle}d(\theta_i,\theta_j) + \frac{\omega_\kappa}{\langle\kappa\rangle}d(\kappa_i,\kappa_j), \tag{9}$$

where $\omega_x + \omega_\theta + \omega_\kappa = 1$. By choosing different values of weights ω_x, ω_θ, ω_κ one can decide which features of the curves are the most important. For example, the following choice of the weights: $\omega_x = \frac{1}{2}$, $\omega_\theta = \frac{1}{4}$ and $\omega_\kappa = \frac{1}{4}$ indicates that in the resulting clustering the radii of the objects are more important than their shapes.

4.2. Dynamic Time Warping (DTW)

In the present section we describe the similarity measure based on the dynamic time warping technique (DTW). In our Schemes, provided later on in this section, we use this technique to measure similarity between functions $\theta(s)$ and $\kappa(s)$, the values of which are sampled at equidistant points of s.

In view of this, the compared functions X and Y are represented by the sequences $X := (x_1, x_2, ..., x_N)$ of length $N \in \mathbb{N}$ and $Y := (y_1, y_2, ..., y_M)$ of length $M \in \mathbb{N}$, respectively, i.e., $X \in \mathbb{R}^N$, $Y \in \mathbb{R}^M$.

In the following, by F we denote the feature space, i.e., $x_n, y_m \in F$ for $n \in [1; N]$, $m \in [1; M]$. To compare two different elements $x, y \in F$, one needs

a local cost measure, sometimes also referred to as the local distance measure, which is defined to be a function

$$c : F \times F \to \mathbb{R}_+. \tag{10}$$

Evaluating the local cost measure for each pair of elements of the sequences X and Y, one obtains the cost matrix $C \in \mathbb{R}^{N\times M}$, defined by $C(n, m) := c(x_n, y_m)$.

An (N, M)-warping path $p = (p_1, ..., p_L)$ is defined by an alignment between two sequences: $X = (x_1, x_2, ..., x_N)$ and $Y = (y_1, y_2, ..., y_M)$, this alignment being obtained by assigning the element x_{n_l} of X to the element y_{m_l} of Y . The total cost $c_p(X, Y)$ of a warping path p between X and Y with respect to the local cost measure c is defined as

$$c_p(X, Y) := \sum_{\ell=1}^{L} c(x_{n_l}, y_{m_l}). \tag{11}$$

The next definition formalizes the notion of a warping path.

Definition 1 *An (N,M)-warping path (simply referred to as warping path if N and M are clear from the context) is a sequence $p = (p_1, ..., p_L)$ with $p_\ell = (n_\ell, m_\ell) \in [1 : N] \times [1 : M]$ for $\ell \in [1 : L]$ satisfying the following three conditions:*

(i) Boundary condition: $p_1 = (1, 1)$ and $p_L = (N, M)$.
(ii) Monotonicity condition: $n_1 \le n_2 \le ... \le n_L$ and $m_1 \le m_2 \le ... \le m_L$.
(iii) Step size condition: $p_{\ell+1} - p_\ell \in \{(1, 0), (0, 1), (1, 1)\}$ for $\ell \in [1 : L - 1]$.

An optimal warping path between X and Y is a warping path p^* having minimal total cost among all possible warping paths. The DTW distance $dtw(X, Y)$ between X and Y is then defined as the total cost of p^*:

$$DTW(X, Y) := c_{p^*}(X, Y) = \min\{c_p(X, Y) \mid p \text{ is an } (N, M)\text{-warping path}\} \tag{12}$$

In our approach, we calculate DTW distance between the tangent functions $\theta(s)$, and the curvature functions $\kappa(s)$ of a pair of curves. Let M be the number of curves in the considered set. We define the weighted d_{DTW} sum distance as follows. For any curve i and j we put:

$$d_{DTW}(i, j) = \frac{\omega_x}{\langle\langle x\rangle\rangle}|x_r^i - x_r^j| + \frac{\omega_\theta}{\langle\langle\theta\rangle\rangle}DTW(\theta_i, \theta_j) + \frac{\omega_\kappa}{\langle\langle\kappa\rangle\rangle}DTW(\kappa_i, \kappa_j), \tag{13}$$

where $\langle\langle x\rangle\rangle$, $\langle\langle\omega\rangle\rangle$, $\langle\langle\kappa\rangle\rangle$ are normalized factors defined as follows

$$\begin{aligned}\langle\langle x\rangle\rangle &= \tfrac{1}{M}\sum_{i=1}^{M} x_r^i,\\ \langle\langle\Omega\rangle\rangle &= \tfrac{1}{M}\sum_{i=1}^{M} DTW(\theta_i, 0),\\ \langle\langle\kappa\rangle\rangle &= \tfrac{1}{M}\sum_{i=1}^{M} DTW(\kappa_i, 0),\end{aligned}$$

with $\omega_x + \omega_\theta + \omega_\kappa = 1$.

The DTW distance is akin to Fréchet distance, see Aronov, Har-Peled, Knauer, Wang and Wenk (2006); Müller (2007).

4.3. Similarity matrix

By using formula (9) or formula (13), for each pair of curves i, j we calculate the number $d(i,j)$ or $d_{DTW}(i,j)$. These numbers form two similarity matrices D and D_{DTW}, with entries $d(i,j)$ and $d_{DTW}(i,j)$, respectively .

5. The representative functions method

5.1. The fundamental scheme

The literature provides a number of methods based on representative functions (see Gilboa, Karasik, Sharon and Smilansky, 2004; Karasik and Smilansky, 2001, 2008; Sragusti, Karasik, Sharon and Smilansky, 2005).

The points on the curves are specified by their distance along the curves from the predefined reference point i.e. s-arclength, and $s = 0$ is set to be the first lowermost point from the left (the smallest x coordinate among the points, for which the second coordinate is 0, y=0).

To calculate $d(i,j)$ we must **truncate** the domain of s to the largest interval in which the two (or all) functions are defined, and denote its end-points by $[S_{min}, S_{max}]$. The interval $[S_{min}, S_{max}]$ depends on the pair of discrete curves which are compared.

In contrast to this, calculation of $d_{DTW}(i,j)$ does not require truncation of the domain. The corresponding scheme (Scheme DTW) will be proposed in the next subsection.

Below, we recall the Scheme K1, proposed by Karasik and Smilansky (2001); Sragusti, Karasik, Sharon aand Smilansky (2005).

Scheme 1 Scheme K1

[1] Using R1 calculate $x(s)$, $\theta(s)$ and $\kappa(s)$ according to the analytic formulas (5), (6),

[2] Truncate the domains of $x(s)$, $\theta(s)$ and $\kappa(s)$ to the smallest one:

[2a] in the whole set of curves,

[2b] for any pair of functions $x(s)$, $\theta(s)$ and $\kappa(s)$,

[3] Calculate the distance between any two curves according to the formula, (9) with given weights ω_x, ω_θ, ω_κ (which express the importance of features in clustering)

[4] Perform clustering on the basis of the similarity matrix by the standard clustering algorithms.

The following observations, related to the steps of Scheme K1, motivate the modifications, proposed in subsection 5.2 of this original scheme:

Ad 1. It is not necessary to use all the three functions $x(s)$, $\theta(s)$ and $\kappa(s)$ to identify a given curve α.

Ad 2. Truncations of domains to the smallest one in a given set results in a considerable loss of information and, in consequence, leads to perturbation in the classifications.

Ad 3. The discrete integral distance between functions, calculated according to (8), seems to generate proper similarity measure only for sets of objects with domains, which are close to each other.

5.2. The proposed scheme

In the present subsection we propose the following new procedure for clustering of 2D curves, representing cross-sections of rotationally symmetric objects. Relative to Scheme K1 we modify the steps 1-3.

Scheme 2 Scheme DTW

[1] Calculate the radius x_r and the functions $\theta(s)$ and $\kappa(s)$ for every curve in the set of curves according to the formulas given above as formulas (1), (5), (6) (according to R2),

[2] For any two curves calculate the distance between the functions $\theta(s)$ and $\kappa(s)$ according to DTW formulas (11), (12)

[3] Calculate the similarity measure, defined by the DTW weighted sum formula (13),

[4] Perform clustering on the basis of the similarity matrix DTW by a standard clustering algorithm with generation of the respective dendrogram.

*

6. Application - grouping of archeological pottery fragments

In the present section we consider the application of the above schemes in classification of archaeological ceramic fragments. The objects, described by curves as defined in Section 2 are cross-sections of vessels or their fragments, uncovered in the course of archaeological work. When dealing with archaeological ceramics, cross-sections are referred to as *profiles*. We consider the pottery fragments belonging to one of the two following types:

1. *rims* - the top part of the vessel
2. *full profile* - a profile of a vessel, which is preserved from the rim to the base.

The drawings of sections come from hand-made drawings. As these drawings belong to the class of technical drawings, they are made according to a set of rules and use conventions, as well as a visual language, in order to maintain standards and convey as much information about a vessel or a fragment as possible, without the need to supplement it with text. This, in turn, allows

for making an automated or semi-automated comparison between the drawings. And so the vertical line in the middle denotes the rotation axis. The great majority of vessels have a rounded form (when formed on a potter's wheel), which means that a section and the location of the rotation axis are sufficient to convey the shape of the vessel. The distance between the rotation axis and the rim denotes the radius of the vessel. It is worth mentioning that there exist methods for automatic generation of the profiles of pottery fragments from 3D scans, see Cao and Mumford (2002) and the references therein.

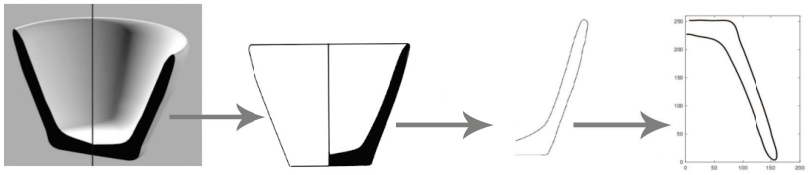

Figure 5: The transformation of a section of a vessel into a 2D curve

The classification of pottery, obtained through excavations, is an important part of archaeological analysis. It is a form of organizing the material for purposes of drawing conclusions concerning the investigated sets, which can be very large at times (up to thousands of items). Such classifications are traditionally performed manually and are based usually on drawings of the vessels and their fragments. These manually created classifications depend heavily on the researchers' knowledge and experience and are, therefore, prone to being bia-sed. An automatic realization of these tasks leads to more objective results and speeds up the process. During the process of classification, the vessels can be divided into groups based on many features. In this paper, we consider as features size, global shape and local shape.

The problem of automatic and semi-automatic classification of ceramic fragments has been investigated by a number of authors. In Piccoli et al. (2015) two complementary approaches to automatic classification of archaeological fragments are presented: one that focuses on medial points of the fragment profiles and the second, focusing on visual features of the fragment surface. Maiza and Gaildrat (2005) consider, in turn, other profile base automated pottery classification approaches. Gilboa, Karasik, Sharon and Smilansky (2004) developed a mathematical and numerical tool for morphological description, classification and analysis of archaeological fragments. Yet other approaches to classification of pottery fragments are presented in Hristov and Agre (2013), Kampel and Sablatnig (2000), Kampel, Sablatnig and Costa (2001), Karasik and Smilansky (2001), Makridis and Daras (2013), Sablatnig, Menard and Kropatsch (1998), and Smilansky et al. (2010).

The starting point for our analysis is the classification method, based on representative functions, as proposed in Karasik and Smilansky (2001).

7. Experiment

In order to test our method we have designed and conducted an experiment. To that purpose we have chosen 35 profiles of vessels (SET 1). The profiles used for the experiment come from the publication by P. Mountjoy (1999), and represent a selection of few types of the Late Helladic vases.

The experiment was conducted according to two schemes, described above. The results are considered as good when they coincide with the traditional classification, published in Mountjoy (1999).

7.1. Description of the tested data set

The set is composed of 35 curves, representing rims and full profiles of varying types (Fig. 6).

According to the traditional classification (typology) presented in Mountjoy (1999), they represent five groups of vessels:

1. Alabastra (1, 2, 3, 4, 5, 6, 7) - marked as **a** in dendrograms,
2. Amphoriskoi (8, 9, 10, 11, 12, 13, 14) -marked as **b** in dendrograms,
3. Bowls (15, 16, 17, 18, 19, 20, 21, 22) - marked as **c** in dendrograms,
4. Kraters (23, 24, 25, 26, 27, 28) - marked as **d** in dendrograms,
5. Lekytoi (29, 30, 31, 32, 33, 34, 35) - marked as **e** in dendrograms.

Among those fragments there are 28 full profiles and 7 rim fragments. Figure 6 shows the collective profiles of the the five groups of vessels, used in the experiment. The alabastra (Fig. 7a) are relatively small vessels, with a square shaped body, narrow neck and tall rim, turned outwards with a convex base. The amphoriskoi (Fig. 7b) are close to the alabastra, being small vessels, with a narrow neck and an outward turned rim. Contrary to alabastra, they have a rounded body and a usually concave base with a foot. Alabastra have some variation when it comes to the height of the vessels. The bowls (Fig. 7c) have a varied height within the group. They are open vessels with a curved body, a base with a foot, the rim is less turned outwards that in the alabastra and the amphoriskoi. What distinguishes the fourth group, the kraters (Figure 7d), from the other groups is the size, both in terms of height and rim diameter. In terms of shape, kraters are akin to bowls, with a more elongated body. The last group, the lekythoi (Fig. 7e), are jug-like vessels with a tall, narrow neck, rounded body, and a concave base with a foot. They are most akin to amphoriskoi, and they differ by the tall neck. The fifth figure (Fig. 7e) shows the lekytoi compared to a krater, so as to show the difference in size between the vessel groups. The five groups have been chosen as very distinctive, although they share some characteristics, such as the shape of the rim (amphoriskoi and lekytoi), size (alabastra and amphoriskoi), or general shape (bowls and kraters). This choice of profiles for the experiment will allow us to accurately show how the method performs. The profiles chosen for the experiment represent at least 1/3 of the full vessel profile. This is due to the fact that the inclusion of very short fragments in the classified set usually leads to erroneous results, as they provide too little information to be properly classified.

7.2. Scheme K1

This Scheme is a version of the method proposed in Karasik and Smilansky (2001), and Gilboa, Karasik, Sharon and Smilansky (2004). The comparison between respective functions is done pairwise. As mentioned above, pairwise comparisons rely on establishing a common domain for each pair of profiles separately, instead of establishing a common domain for the whole set. Intuitively, it is clear that pairwise comparisons should be more appropriate in case the set of classified objects contains curves of varying length. Our experiment supports this intuitive conviction.

We performed experiments with the following weights:

1. $\omega_x = 1/3$, $\omega_\theta = 1/3$, $\omega_\kappa = 1/3$
2. $\omega_x = 1/2$, $\omega_\theta = 1/4$, $\omega_\kappa = 1/4$
3. $\omega_x = 1/4$, $\omega_\theta = 1/2$, $\omega_\kappa = 1/4$
4. $\omega_x = 1/4$, $\omega_\theta = 1/4$, $\omega_\kappa = 1/2$.

The third choice of the weights, $\omega_x = 1/4$, $\omega_\theta = 1/2$, $\omega_\kappa = 1/4$, leads to the results, which are the closest to the traditional classification, as given in Mountjoy (1999). As seen in Fig. 8, these results are far from satisfactory. The group of kraters stands out from the rest of the set, being the best classified group. Their overwhelming difference in size, when compared to the other four groups, seems to be decisive here, even though it is the function responsible for the general shape that was given the highest weight. The group of alabastra is reasonably well classified, aside from profile 2. Profile 2 has been placed away from its, group because of its different rim (the uppermost part), which is different from the others in the group. This shows how a small change in the shape can disturb the classification. The change in the rim overshadows the correspondence in the shape of the body of the vessel. This is due to the points on the curve being compared with respect to their subsequent numbers, which means that a shift in the numbers ("longer" rim) leads to the lack of correspondence between the points when the body part is compared. The other three groups are mixed together and the degree, to which they are grouped is unsatisfactory. Profile 19 is placed outside of all the groups. This is probably due to the fact that profile 19 is considerably shorter than the others. In archaeological terms, we interpret this as profile 19 possibly belonging to any of the groups a, b, c or e, but not to group d.

In order to fully investigate the representative functions method, we have performed an experiment using the same scheme, but truncating the domain to the smallest one in the set. As in the previous case, the group of kraters is well pronounced. Apart from the kraters, only the bowls are fairly well grouped together. Other groups are mixed and no clear structure of the data is discernible. This can be attributed to the truncation process, as the smallest fragment, profile 19, is very short, when compared to the other fragment. The kraters have been properly classified, as their large size outweighs other aspects of the shape, whereas the bowls have a very distinctive rim, when compared to other groups. Because of the truncation, there was not enough data left,

concerning the shape, to perform a satisfactory classification.

7.3. Scheme DTW

In order to overcome the shortcomings of Scheme K1, discussed above, we have decided to apply the Dynamic Time Warping (DTW) algorithm for calculating distances, in order to compare the representative functions. For purposes of improving the efficiency of the algorithm, we decided to substitute the arc length function $x(s)$ with a single number x_r, as described in (1).

As in the case of Scheme K1, experiments with several weights have been conducted. Also in this case the best results were obtained for weights $x_r = 1/4$, $\omega_\theta = 1/2$, $\omega_\kappa = 1/4$. The results are presented in Fig. 10. In this classification the groups are concise and clearly delineated. This result also shows the structure of the data, i.e. the relations between the groups. The closest resemblance is shown to exist between alabastra and amphoriskoi. Together, they are akin to lekytoi, as all these vessels have a narrow opening, and a more or less pronounced neck. These three groups differ from bowls, which are open shape vessels. Similarly as previously, profile 19 could belong to either of the groups, as there is too little information about it to classify it surely to one distinctive group. Such a result is acceptable, as it mimics the situations that occur in real life. The group that shares very little similarity with the others are the kraters. The method performs correctly, thanks to the use of the DTW algorithm for the comparison of the functions. The DTW provides the necessary flexibility in comparing the functions. This allows for the characteristic points being well matched and favours the matching of shape features, expressed as functions, rather than just the points with corresponding indices.

It is worth mentioning that the methods were tested on other data sets of similar size to the one presented here. Every time the results were satisfactory. The tables below summarize the experiments carried out. Experiments were preformed on Set 1 (described in 7.1) and two other sets.

Table 1: Structure of sets used in experiments: number of profiles, number of points in the profile of minimal length and number of points in the profile of maximal length

	Number of profiles	Min length	Max length
SET 1	35	276	2553
SET 2	30	3122	13 211
SET 3	32	1290	5955

8. Conclusions

In conclusion, the proposed method performs well for sets of profiles of vessels coming from the field of archaeological research. Such method, although not

Table 2: Percent of misclassified profiles in each scheme and set

	Scheme K1 with 2b	Scheme DTW
SET 1	45.7%	2.8%
SET 2	43.3%	23.3%
SET 3	9.4%	0%

Table 3: Total execution time in seconds for each scheme and set

	Scheme K1 with 2b	Scheme DTW
SET 1	6.261	13.435
SET 2	12.869	133.031
SET 3	11.890	130.663

conclusive, is of great assistance to archaeologists, who are dealing with large sets of ceramic material. While it requires the knowledge of the scientists to calibrate it properly, it facilitates the mundane task of pottery classification.

The future challenge is to test the method on significantly larger sets. So far we have been working only with profiles of the whole vessel or rim fragments. As a part of our further research we plan to investigate profiles of fragments that are the lower part of the vessel, i.e. the base. Another problem arises when the investigated vessel has a handle. As far as we know, this problem has not yet been addressed in literature. The presented problem can be also approached as the clustering of silhouettes. Furthermore, an angle that we find worth further investigation, is to look at our problem from the perspective of machine learning methods.

References

AMANATIADIS, A., KABURLASOS, V.G, GASTERATOS A., and PAPADATIS, S.E. (2011) Evaluation of shape descriptors for shape-base image retirieval. *IET Image Process, Special issue on Imaging Systems and Techniques* **5** (5), 493–8499.

ARICA, N. and YARMAN-VURAL, F.T. (2003) A Compact Shape Descriptor Based on the Beam Angle Statistics. *Image and Video Retrieval*, Springer, 152–162.

ARONOV, B., HAR-PELED, S., KNAUER, C., WANG, Y. and WENK, C. (2006) *Fréchet Distance for Curves, Revisited*. Springer, Berlin Heidelberg.

BANDYOPADHYAY, S. and SAHA, S. (2013) Unsupervised Classifcation. *Similarity Measures, Classical and Metaheuristic Approaches, and Applications*. Springer, Berlin Heidelberg.

BELONGIE, S. and MALIK, J. (2000) Matching with Shape Context. *IEEE Workshop on Contentbased Access of Image and Video Libraries (CBAIVL-2000)*, IEEE Pubs., 20–26.

BELONGIE, S. and MALIK, J. (2002) Shape Matching and Object Recognition Using Shape Context. *IEEE Transactions on Pattern Analysis and Machine Intelligence* **24** (24), 483–507.

BINKOWSKI, T. A. and JOACHIMIAK, A. (2008) Protein functional surfaces: global shape matching and local spatial alignments of ligand binding sites. *BMC Structural Biology* **8** (1).

BRIDLE, J. S. (1980) Pattern recognition techniques for speech recognition. *Spoken Language Generation and Understanding*, Springer Netherlands, Dordrecht, 129–145.

CAO, F. (2003) Geometric curve evolution and image processing. *Lecture Notes in Mathematics* **1805**. Springer.

CAO, Y., and MUMFORD, D. (2002) Geometric structure estimates of axially symmetric pots from small fragments. *Proc. of Int. Conf. on Signal Processing, Pattern Recognition and Applications*. IASTED, 92-97.

DO CARMO, M. P. (1976) *Differential Geometry of Curves and Surfaces*. Prentice Hall, Inc., Englewood Cliffs, New Jersey.

FORSYTH, D.A, MUNDY, J.L., DI GESU, V. and CIPOLLA, R. (1999) *Shape, Contour and Grouping in Computer Vision. Lecture Notes in Computer Science* **1681**, Springer-Verlag, Berlin Heidelberg.

GARCÍA-ORDÁS, M.T., ALEGRE, E., GARCÍA-OLALLA, O. and GARCÍA-ORDÁS, D. (2013) Evaluation of different metrics for shape based image retrieval using a new contour points descriptor. *Similarity Search and Applications: 6th International Conference, SISAP 2013, A Coruña, Spain, October 2-4, 2013, Proceedings*. Springer Berlin Heidelberg, 141–150.

GHOSH, D., DUBE, T. and SHIVAPRASAD, A.P. (2010) Script recognition – a review. *IEEE Trans Pattern Anal Mach Intell* 32 (12), 2142–2161.

GILBOA, A., KARASIK, A., SHARON, I. and SMILANSKY, U. (2004) Towards computerized topology and classification of ceramics. *Journal of Archaeological Science* **35**, 1148–1168.

HRISTOV, V. and AGRE, G. (2013) A software system for classification of archaeological artefacts represented by 2D plans. *Cybernetics and Information Technology* **13** (2), 82–96.

KAMPEL, M. and SABLATNIG, R. (2002) Computer aided classification of ceramics. In: F. Nicolucci, ed., Virtual Archaeology. Proc. of VAST 2000 Euroconference, Arezzo,. Oxford, *BAR*, International Series, 77–82.

KAMPEL, M., SABLATNIG, R. and COSTA, E. (2001) Classification of archaeological fragments using profile primitives. In: S. Scherer, ed., *Computer Vision, Computer Graphic and Photogrammetry - a Common Viewpoint. Proceedings of 25th AAPR Workshop*, Schrifttenreihe der OCG, *147* 151–158.

KARASIK, A. and SMILANSKY, U. (2001) Computerized morphological classification of ceramics. *Journal of Archaeological Science* **38**, 2644–2657.

KARASIK, A. and SMILANSKY, U. (2008) 3D scanning technology as a standard archaeological tool for pottery analysis: Practice and theory. *Journal of Archaeological Science* **35** (5), 1148–1168.

KIMMEL, R., SHAKED, D., KIRYATI, N. and BRUCKSTEIN, A.M. (1995)

Skeletonization via distance maps and level sets. *Computer Vision and Image Understanding* **62** (3), 382–391.

KOVALEVSKY, V. (2001) Curvature in digital 2D images. *International Journal of Pattern Recognition and Artificial Intelligence* **15**, 1183–1200.

LIU, H., LATECKI, L.J. and LIU, W. (2008) A unified curvature definition for regular, polygonal, and digital planar curves. *International Journal of Computer Vision* **80**, 104–124.

MAIZA, C. and GAILDRAT, V. (2005) Automatic classification of archaeological potsherds. *The Eight th International Conference on Computer Graphics and Artificial Intelligence, 3IA'2005* , 11–12.

MAKRIDIS, M. and DARAS, P. (2013) Automatic classification of archaeological pottery sherds. *J. Comput. Cult. Herit.* **5** (4), 15:1–15:21.

MASOOD, A. and SARFRAZ, M. (2008) An efficient technique for capturing 2D objects. *Computers & Graphics* **32**, 93–104.

MASOOD, A. and SARFRAZ, M. (2009) Capturing outlines of 2d objects with bézier cubic approximation. *Image and Vision Computing* **27** (4), 704–712

MÜLLER, M. (2007) *Information Retrieval for Music and Motion.* Springer Science & Business Media.

MOUNTJOY, P. A. (1999) *Regional Mycenaean Decorated Pottery.* Marie Leidorf.

MUMFORD, D.(1991) Mathematical theories of shape: do they model perception? In: *Proc. Conference 1570, Soc. Photo-optical & Ind. Engineers (SPIE)*, 2–10.

PAL, S., GANGULY, P. and BISWAS, P.K. (2007) Cubic Bézier approximation of a digitized curve. *Pattern Recognition*, **40**, 2730–2471.

PARRACHO, P., NEVES, R. and HORTA, N. (2010) Trading in Financial markets using pattern recognition optimized by genetic algorithms. In:*Proceedings of the 12th Annual Conference Companion on Genetic and Evolutionary Computation, GECCO '10*, 2105–2106, ACM, 2010.

PICCOLI, C., APARAJEYA, P., PAPADOPOULOS, G. TH., BINTLIF, J., LEYMARIE, F., BES, P., POBLOME J., VAN DER ENDEN, M. and DARAS, P. (2015) Towards the automatic classification of pottery sherds: two complementary approaches. In: *Across Space and Time. Papers from the 41st Conference on Computer Applications and Quantitative Methods in Archaeology*, 463–474.

RAMSAY, J.O. and SILVERMAN, B.W. (2002) Functional Data Analysis. Methods and Case Studies. Springer.

RUI, Y., SHE, A. C. and HUANG, T. S. (1996) Modified Fourier descriptors for shape representation – a practical approach, In: Proc. of First International Workshop on Image Databases and Multi Media Search. Amsterdam, The Netherlands.

SABLATNIG, R., MENARD, CH. and KROPATSCH, W. (1998) Classifcation of archaeological fragments using a description language. In: *Proceedings of European Association for Signal Processing (Eusipco) 1998, Island of Rhodos, Greece* **2**, 1097–1100.

SARAGUSTI, I., KARASIK, A., SHARON, I. and SMILANSKY, U. (2005) Quantitative analysis of shape attributes based on contours and section profiles in artefact analysis. *Journal of Archaeological Science*, **32**, 841–853.

SARFAZ, M. and MASOOD, A. (2007) Capturing outlines of planar images using Bézier cubics. *Computers & Graphics*, **31**, 719–729.

SARFAZ, M., MASOOD, A. and ASIM, R. (2004) A web based system for capturing outlines of 2d objects. In: *Proceedings of International Conference on Information & Computer Science, Dhahran, Saudi Arabia*, 177–193.

SEBASTIAN, T., KLEIN, P. and KIMIA, B. (2003) On aligning curves. *IEEE trans. Pattern Anal. Machine Intell.*, **25**(1), 116–125.

SHARON, E. and MUMFORD D. (2006) 2D-shape analysis using conformal mapping. *International Journal of Computer Vision*, **70**(1), 55–75.

SMILANSKY, U., BEIT-ARIEH, I., KARASIK, A., SHARON, I. and GILBOA, A. (2010) Optimal choice of prototypes for ceramic typology. In: F. Nicolucci and S. S. Hermon, eds., *Beyond the Artifact. Digital Interpretation of the Past. Proceedings of CAA2004, Prato 13–17 April 2004*, 411–414.

KŁOPOTEK, M.A. and WIERZCHOŃ, S.T. (2015) *Algorithms of Cluster Analysis*. Instytut Podstaw Informatyki PAN.

WYLIE, T. (2013) The Discrete Fréchet Distance with Applications. PhD thesis, Montana State University.

WYLIE, T. and ZHU, W.B. (2014) Intermittent Map Matching with the Discrete Fréchet Distance, arXiv:1409.2456

YADAV, P. and YADAV, N. (2015) Handwriting Recognition System - A Review. *International Journal of Computer Applications*, **114**(19), 36–40.

ZHANG, D. and LU, G. (2003) Evaluation of MPEG-7 shape descriptors against other shape descriptors. *Multimedia Systems*, **9**, 15–30.

ZHANG, D. and LU, G. (2004) Review of shape representation and description techniques. *Pattern Recognition*, **37**(1), 1–19.

ZHANG, D. and LU, G. (2002) A comparative study of Fourier descriptors for shape representation and retrieval. In: *Proc. of 5th Asian Conference on Computer Vision (ACCV)*, Springer, 646–651.

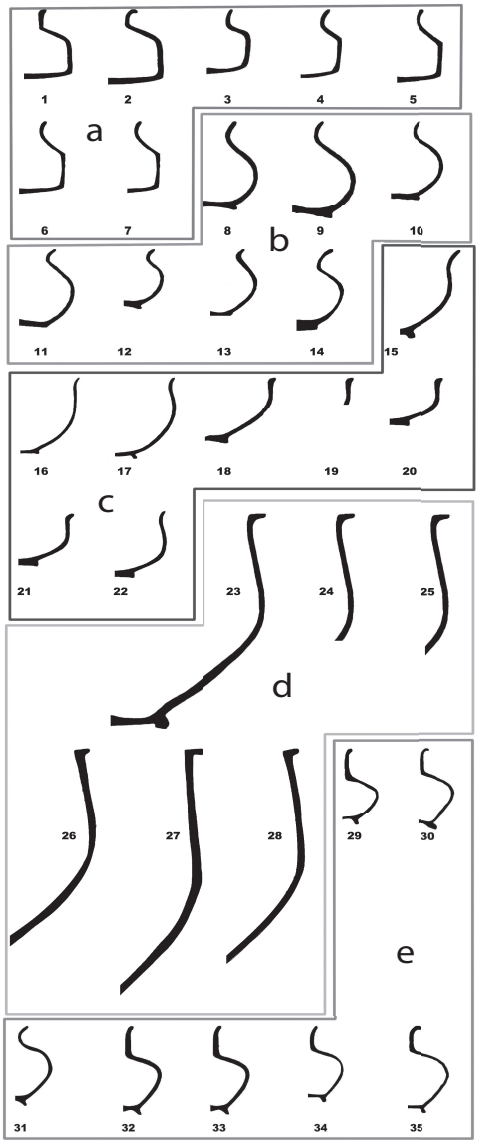

Figure 6: The investigated set of profiles (all in the same scale)

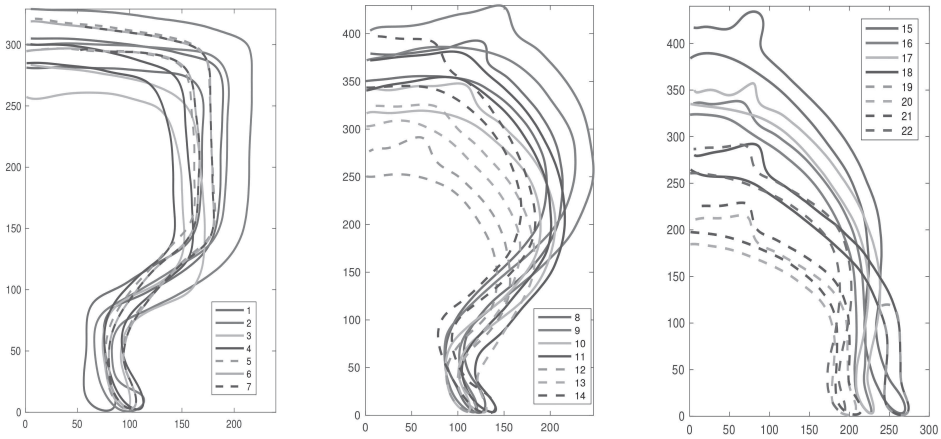

(a) Alabastra (b) Amphoriskoi (c) Bowls

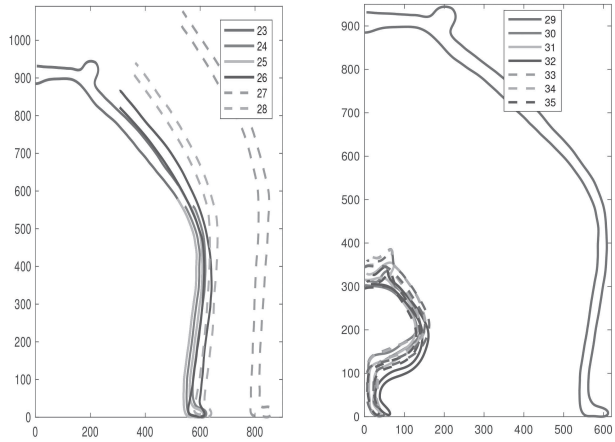

(d) Kraters (e) Lekytoi

Figure 7: Five groups of vessels

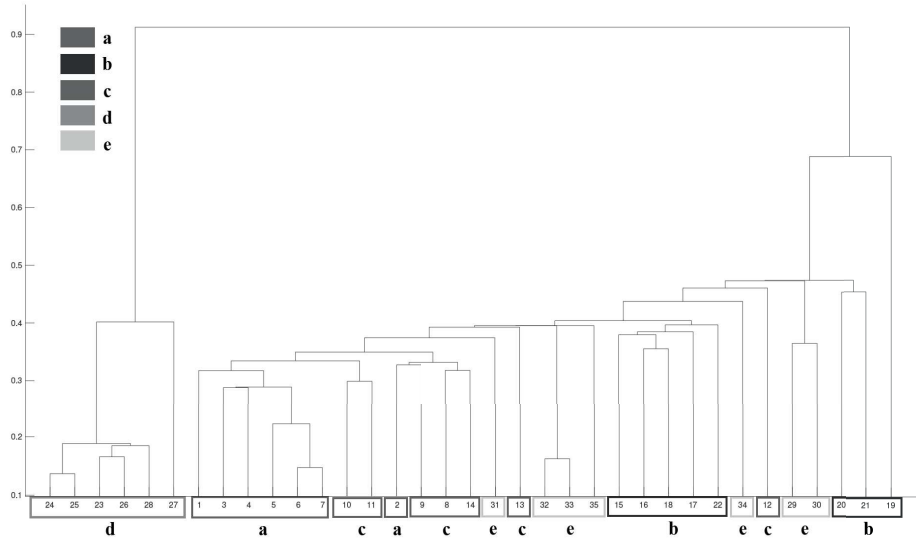

Figure 8: Classification result obtained using Scheme K1 with pairwise truncation of domains with weights $\omega_x = 1/4$, $\omega_\theta = 1/2$, $\omega_\kappa = 1/4$

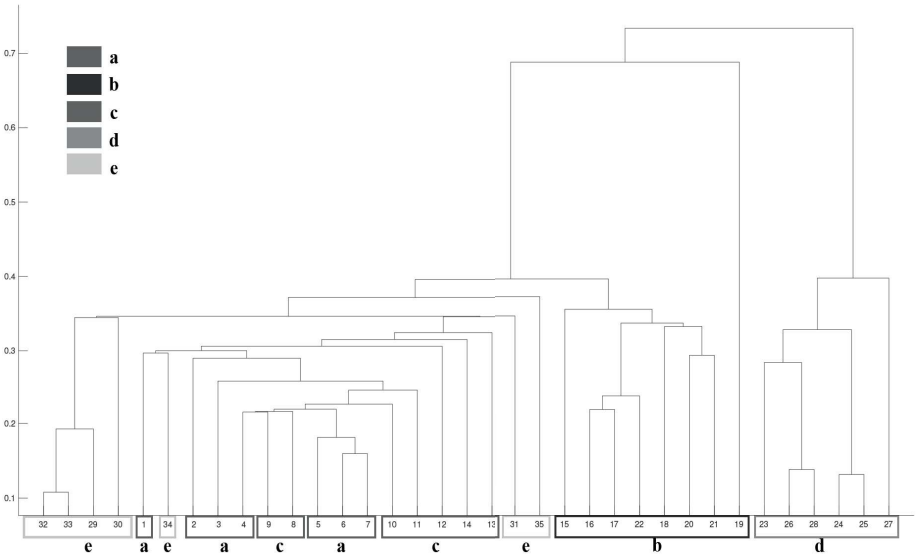

Figure 9: Classification result obtained using Scheme K1 with the truncation of the domains to the smallest one in the set, with weights $\omega_x = 1/4$, $\omega_\theta = 1/2$, $\omega_\kappa = 1/4$

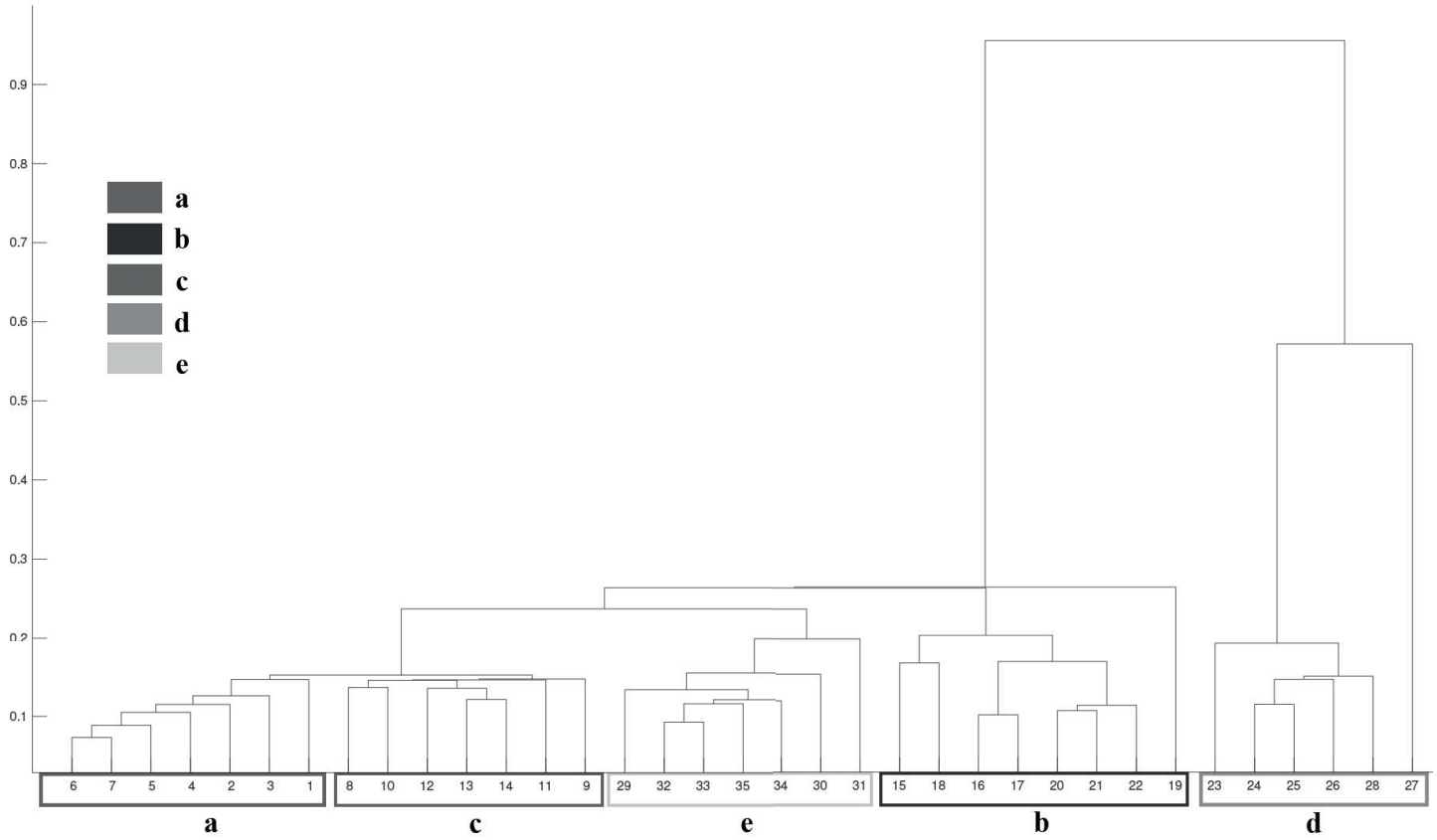

Figure 10: Classification result obtained using Scheme DTW with weights $\omega_x = 1/4$, $\omega_\theta = 1/2$, $\omega_\kappa = 1/4$